Appl. Phys. B 61, 529–532 (1995)

Applied Physics B Lasers and Optics

Rapid communication

Collinear and non-collinear sum-frequency mixing in β-BBO for a tunable 195–198 nm all-solid-state laser system

J. Lublinski[1], M. Müller[1], F. Laeri[1,*], K. Vogler[2]

[1] TH-Darmstadt, Institute of Applied Physics, Schlossgartenstrasse 7, D-64289 Darmstadt, Germany
(Fax: +49-6151/163022, E-mail: FRANCO.LAERI@physik.th-darmstadt.de)
[2] Aesculap-Meditec, D-90562 Heroldsberg, Germany

Received: 4 June 1995 / Accepted: 22 August 1995

Abstract. We attained tunable UV laser radiation between 195 and 198 nm by sum-frequency mixing two synchronized flashlamp-pumped solid-state Q-switch lasers, a Nd:YAG laser frequency quadrupled to 266 nm and a tunable (730–770 nm) alexandrite laser. UV pulse energies of 0.12 mJ with repetition rates of 10 Hz were attained in collinear, as well as non-collinear sum-frequency interaction in a β-Barium Borate (BBO) crystal with a conversion efficiency of 2.5%. Theoretical models for the non-collinear phase-matching interaction were investigated at UV wavelengths below 200 nm.

PACS: 42.50.Ne; 42.55.Rz; 42.60.Jf; 42.60.Mi; 42.65.Ky

Recently numerous novel techniques were developed which require efficient ultraviolet light sources, as, e.g., photolithography, photo-ablation of organic material, or various sorts of photo-stimulation. In addition to efficiency, especially wavelength tunability is an important issue for various procedures of the spectroscopy of atoms and molecules. Below 200 nm the ArF-excimer laser allows the generation of UV radiation with high efficiency, though in a narrow wavelength window around 193 nm. On the other side, compared to solid-state lasers, its beam quality and spectral purity is in general poor. Improvement of those parameters is usually attained with injection seeding techniques [1], thus at the expense of increased complexity and cost of the system. In addition, excimer lasers involve handling of toxic and corrosive fluorine, as well as high-speed high-voltage gas discharges to produce the lasing plasma; aspects which are disfavored in sensitive environments like a surgical operation room. There are, therefore, a number of good reasons to investigate all-solid-state laser concepts for obtaining tunable radiation below 200 nm. Unfortunately no known solid-state laser material emits directly in this wavelength region, so that nonlinear frequency conversion of IR-radiation must be envisioned.

Only few nonlinear crystals exhibit the required phase-matching properties to allow conversion below 200 nm. The first step toward this wavelength range was made by Kato [2]. He attained 196.6 nm in Potassium Penta-Borate tetrahydrate (KB5) by Sum-Frequency Mixing (SFM) the outputs of the fourth harmonic of a Nd:YAG laser together with the output of a near-infrared dye laser. Generation of tunable picosecond pulses in KB5 down to 197 nm as well as continuous-wave radiation at 194 nm were reported in [3, 4]. After the advent of β-Barium BOrate (BBO) and Lithium BOrate (LBO), the attention concentrated on these more efficient crystals. LBO is transparent down to 160 nm, whereas BBO has its cutoff near 189 nm. Borsutzky et al. [5] used the fifth harmonic of a Nd:YAG laser and the output of an IR-Optical Parametric Oscillator (OPO) to attain 188 to 195 nm in LBO. In this range, the phase-matching conditions of BBO are more convenient. Glab and Hessler [6] demonstrated 200 nm generation by adding the 600 nm dye laser output to its second harmonic. Mückenheim et al. [7] described a tunable source (189–197 nm) based on sum-frequency mixing a 780–950 nm dye laser together with 248.5 nm of an excimer laser which at the same time was also used to pump the dye laser. Continuous-wave generation near 194 nm has also been accomplished with BBO [8]. Meguro et al. [9] presented the first pulsed all-solid-state concept with two synchronized laser sources. They used the frequency tripled output of a Ti:Sapphire laser (fundamental: 700–900 nm) pumped by the second harmonic of a Nd:YAG laser, mixed together with the fundamental of a second Nd:YAG laser. The sum-frequency output generated in BBO was tunable from 198 to 300 nm.

In this work, we concentrated on the nonlinear conversion schemes and we report about an alternative all-solid-state approach to attain wavelengths between 195 and 198 nm. The system is based on three conversion steps only, namely sum-frequency mixing of the frequency quadrupled Nd:YAG (4H-YAG) laser output (266 nm) with the fundamental of a synchronized flashlamp-pumped Q-switch alexandrite laser (720–770 nm). As an alternative tunable laser medium at these wavelengths, Ti:Sapphire can also be considered. However, although it can be pumped with flashlamps, its short fluorescence lifetime (3.8 μs compared to 260 μs for alexandrite) makes efficient pumping with conventional flashlamps difficult.

* To whom all correspondence should be addressed

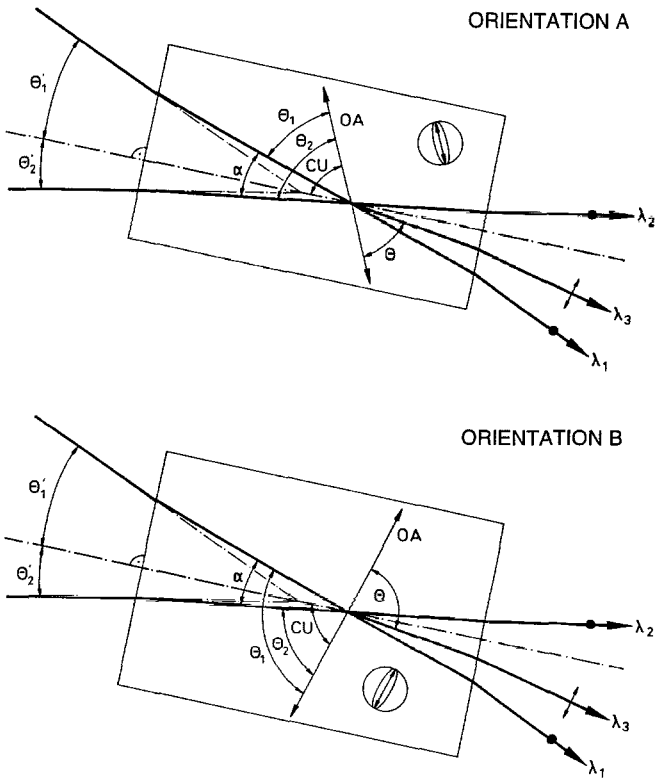

Fig. 1. Definitions of the angles involved in non-collinear SFM; λ_1, λ_2 and λ_3 refer to the alexandrite-beam, the fourth harmonic Nd:YAG and the generated sum-frequency, respectively. The *upper figure* (orientation A) and the *lower figure* (orientation B) represent two possible crystal orientations [cf. text, (3) and (4)]. They correspond to '+' and '∗', respectively in Figs. 4 and 5. Note the polarization direction of the respective beams

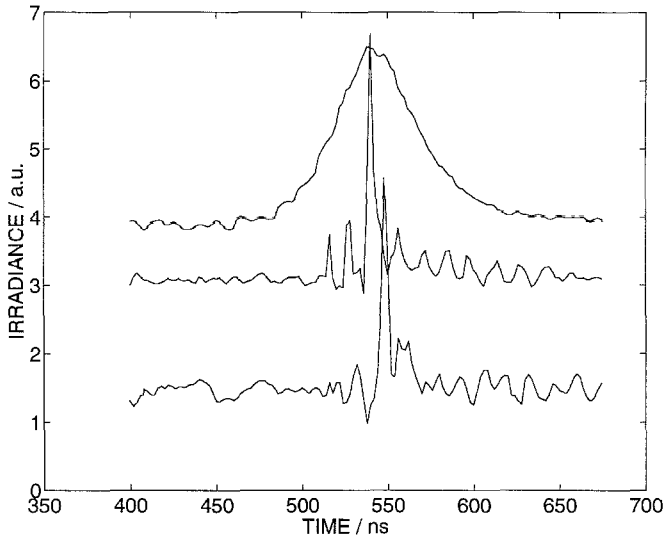

Fig. 2. Pulse shapes of the pumping lasers and the generated sum-frequency; from *top to bottom*: Alexandrite laser pulse (750 nm, 60 ns), fourth harmonic Nd:YAG (266 nm, 4 ns; the wiggles indicate non-perfect suppression of laser spiking) and sum frequency (196.4 nm, 4 ns)

For the nonlinear frequency conversion stages, usually the collinear interaction geometry is considered. On the other side, non-collinear interaction and the associated phase-matching conditions were discussed already in the early 1960s [10]. The most obvious practical advantage of non-collinear SFM is the fact that the two involved pump beams need not to be superposed, and, in the same way, the generated sum needs not to be separated from the pumps after the SFM interaction, so avoiding the optical combining and splitting elements usually needed in the collinear scheme. Especially, if high power pulses are considered in the UV, this is a most favorable feature, since at those wavelengths the optical coatings for the combiners and splitters are rather delicate, easily damaged, fluoride based, and also expensive.

In our experiments, we observed that a non-collinear geometry does not automatically imply a reduced conversion efficiency. On the contrary, it is reported that in some cases the effective nonlinear susceptibility might even turn out to be enhanced [11]. In addition, non-collinear phase matching allows the optimization of further parameters. Dou et al. [12, 13] discuss non-critical properties in non-collinear phase matching. They point out that it is possible to optimize crystal length and beam walkoff in a non-collinear geometry, especially if one of the beams is divergent. Hofmann et al. [15] generated 193 nm by SFM and they propose a spectrally compensated scheme for ultrashort pulses. Also, in femtosecond applications parametric gain is predicted to be larger for those phase-matched directions, which, at the same time, best satisfy group-velocity matching [16]. Further advantages of non-collinear phase matching for optical parametric oscillation were pointed out by [14, 17].

A detailed analysis of non-collinear geometry in BBO was given by Bhar [18]. They introduced a simplified, straightforward method for calculating the phase-matching conditions in uniaxial crystals and verified the model by mixing 1064 nm Nd:YAG laser radiation with visible dye laser radiation of 550-740 nm [19, 20]. In the work presented here, we examined the validity of their model in the UV region below 200 nm. Figure 1 shows the interaction geometry used in the experiments and defines the angles involved in the non-collinear phase-matching geometry. With θ we refer to the phase matching angle ($\theta \leq 90°$) which is defined as the angle between the generated beam and the optical axis, and α denotes the non-collinear angle between the two pump beams inside the crystal. External (dashed symbols) and internal angles are related via the crystal cut angle CU by Snell's law as:

$$\sin\theta_i' = n_i \sin(CU - \theta_i), \qquad i = 1, 2\,. \tag{1}$$

The experiments were performed with a Q-switched alexandrite laser which was synchronized with a frequency-quadrupled Nd:YAG laser. Both were operated at a repetition rate of 10 Hz. The jitter of the synchronizing electronics of ca. 10 ns as well as the inherent optical pulse-to-pulse jitters of both lasers (alexandrite: 20 ns, 4H-YAG: 0.5 ns) were absorbed in the length of the alexandrite pulse of 60 ns.

In Fig. 2, it can be seen that the sum-frequency pulse inherits the length of the shorter of both pump pulses, i.e., the 4H-YAG laser pulse. The sum-frequency pulse is plotted with a delay of ca. 6 with in respect to the pumps, which is a result of additional optical and cable propagation delays in the respective detection channel. As detectors we used fast silicon PIN photo diodes with a rise-time of ca. 0.5 ns. Because of the relatively small stimulated emission cross section of the transition, alexandrite Q-switch pulses shorter than 50 ns are difficult to obtain. A short resonator design is therefore important, although this usually tends to reduce

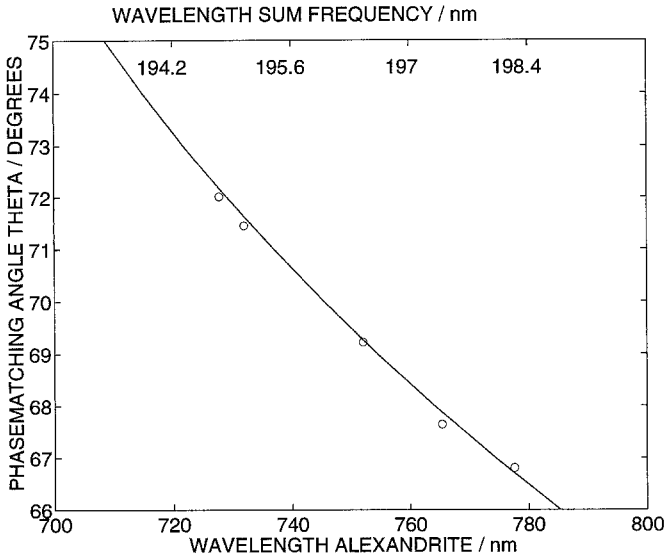

Fig. 3. Collinear phase-matching conditions. *Vertical axis*: Phase-matching angle θ. *Horizontal axis*: Wavelength of the alexandrite laser and the corresponding generated wavelength. The *solid line* represents the theoretical model and the *circles* mark our experimentally obtained angles

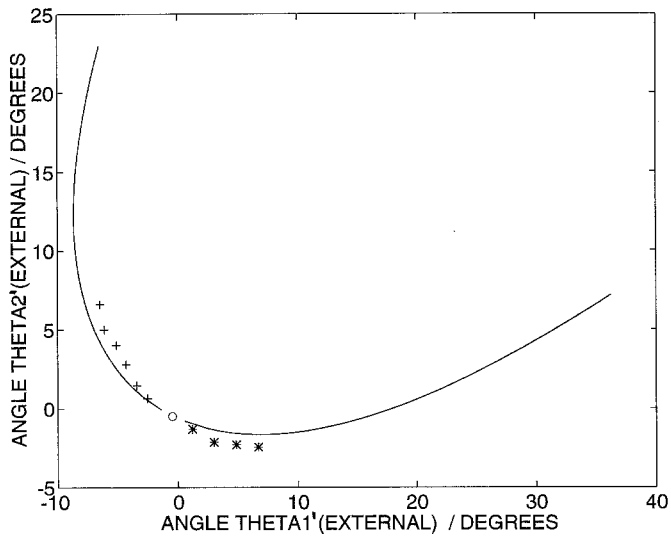

Fig. 4. Representation of the non-collinear phase-matching conditions referred to external angles; θ_1' and θ_2' are the angles of incidence of the alexandrite beam and the frequency-quadrupled Nd:YAG-beam, respectively. The *solid line* represents the theoretical curve. '+' and '$*$' show experimentally obtained results for orientation A and B respectively (Fig. 1), and 'o' marks the collinear case

the achievable mode volume and thus energy extraction as well. In addition, for frequency conversion in nonlinear crystals a smooth transversal mode profile is beneficial. Thus, the alexandrite laser was based on a stable, compact, half-symmetric resonator with a length of 40 cm, containing a Brewster Pockels-cell, a pinhole, and a birefringent tuner. The output energy was 20 mJ, the beam diameter 2.0 mm, and the linewidth ca. 0.1 nm. For the 4H-YAG, we used a Quantel-Brilliant with 30 mJ output at 266 nm. With a Galilean telescope ($f_1 = 400$ mm, $f_2 = -200$ mm), we reduced the output beam diameter of this unstable resonator by a factor of ca. 2 to approximately 2.6 mm. The BBO-crystal ($5 \times 5 \times 7$ mm^3) was 70° cut. The uncertainty of the cut is estimated to be ca. 1°. We attained 0.12 mJ of sum

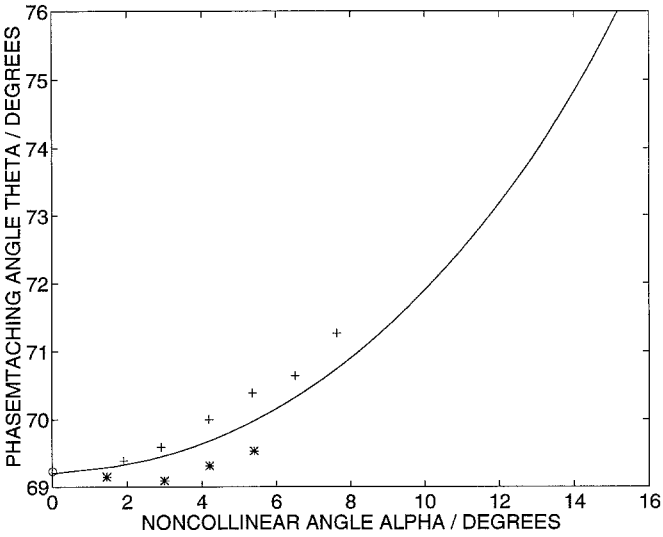

Fig. 5. Measurement of the non-collinear phase-matching conditions given by the (internal) phase-matching angle θ in dependence of the (internal) non-collinear angle α (Fig. 1). Again, '+' and '$*$' refer to orientation A and B, respectively, and 'o' to the collinear case

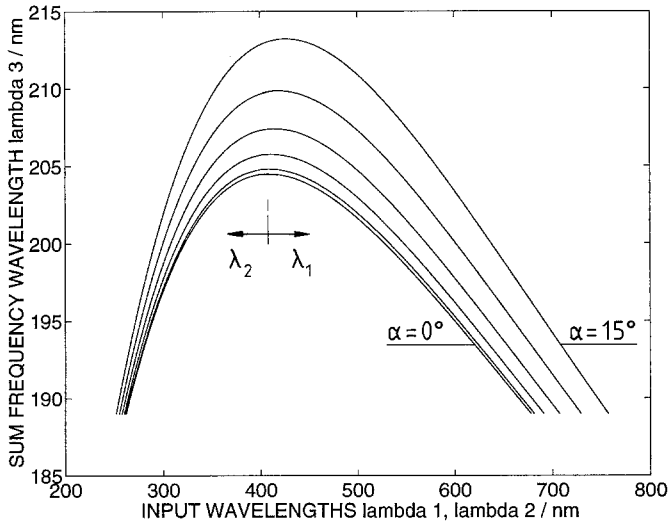

Fig. 6. Representation of wavelength pairs (λ_1, λ_2) for collinear and non-collinear phase matched sum-frequency generation (θ = 90°) in BBO calculated according the model given in [18]. α refers to the non-collinear angle (inside the crystal), cf. Fig. 1; from top to bottom: α = 15°, 12°, 9°, 6°, 3°, 0°. The lowest curve thus marks the collinear non-critical phase matching condition

frequency 196 nm output at 10 Hz repetition rate. This leads to a SFM conversion efficiency in terms of power density η of 2.5%, where

$$\eta = \frac{P(\omega_1 + \omega_2)}{P(\omega_1)^{1/2} P(\omega_2)^{1/2}} \,. \tag{2}$$

Figure 3 shows the achieved tuning range measured with a UV-spectrometer and the corresponding phase-matching angle θ for collinear phase-matching ($\alpha = 0$). To investigate the non-collinear phase-matching properties the wavelength of the alexandrite laser was adjusted to 750 nm. We then varied the non-collinear angle α and fitted the crystal orientation θ for maximum SFM output. In order to survey the whole set of possible incidence angles θ_1', the crystal was once illuminated from one side, and then also from the other side, with

the 4H-YAG beam. This was achieved by turning the crystal by 180° around its long edge. These two orientations (A, B) are represented by the two respective pictures in Fig. 1 for which the following set of relations apply:
Orientation A:

$$\theta_2' > 0, \quad \theta_1' < 0, \quad \theta_1 < \theta < \theta_2, \quad \alpha = -\theta_1 + \theta_2 \,. \tag{3}$$

Orientation B:

$$\theta_2' < 0, \quad \theta_1' > 0, \quad \theta_1 > \theta > \theta_2, \quad \alpha = +\theta_1 - \theta_2 \,. \tag{4}$$

In Figs. 4 and 5 the experimental data are indicated by '+' and '∗' for orientation A and B, respectively. The theoretical curves (solid lines) were derived combining

(a) the Sellmeier equations given by Eimerl et al. [21],
(b) the model equation proposed by Bhar and Chaterjee [18]:

$$\frac{\lambda_1}{\theta_1} + \frac{\lambda_1}{\theta_2} = \frac{\lambda_3}{\theta} \,, \tag{5}$$

which is an approximation to (14) presented in [20], and
(c) the equation given by the vectorial triangle of the three wave vectors $\mathbf{k_1}$, $\mathbf{k_2}$ and $\mathbf{k_3}$:

$$\left(\frac{n_1^o}{\lambda_1}\right)^2 + \left(\frac{n_2^o}{\lambda_2}\right)^2 + 2\frac{n_1^o n_2^o}{\lambda_1 \lambda_2}\cos\alpha = \left(\frac{n_3^e(\theta)}{\lambda_3}\right)^2 \,. \tag{6}$$

The experiments were performed with a type-I phase-matching scheme, the polarization of the pump beams being ordinary (refractive indices: n_1^o and n_2^o) and the polarization of the generated sum-frequency beam extraordinary [index: $n_3^e(\theta)$]. In Figs. 4 and 5 a slight, but systematic misfit between the theoretical model and the actual measurements is apparent. We checked model (5) against the more complete version of (14) in [20], but could not find any significant discrepancy in the results for the wavelengths considered here. Thus, we attribute the slight data misfit to a misalignment of the polarization vectors of the incident laser fields, as the orientation of the optical polarization vectors was controlled with an uncertainty of ca. 2°. In the experiments involving the largest non-collinear angles α, the crystal size was about to limit the undisturbed propagation of the beams. Therefore, some scattering might have troubled the conversion conditions as well. Comparing the non-collinear conversion efficiency with the attained collinear conversion efficiency, we could not register any difference between the two cases, which was more significant than the variability in the laser pulses. On the other side, further improvement of the conversion efficiency by focusing into the crystal was prevented by hot spots in the 4H-YAG beam profile and by uncontrolled fast spiking. As is visible in Fig. 2, a large part of the 60 ns alexandrite laser pulse can not couple with the shorter 4 ns 4H-YAG pulse. Obviously, a better matching of the pump pulse lengths would help to increase the conversion efficiency. Under ideal length-matching conditions, and with temporally and spatially smooth beam profiles, conversion efficiencies, (2) around $\eta = 30\%$ appear attainable.

In Fig. 6, we introduce a compact diagram which synoptically renders the interdependence between the set of attainable wavelength pairs and their associated type-I non-collinear SFM phase-matching geometry in BBO for a given phase-matching angle θ. With this figure, we illustrate the possibilities for the interesting case of $\theta = 90°$ which in the collinear ($\alpha = 0°$) case is referred to as non-critical phase matching [12, 13]. Note that the above discussed experiments were performed at phase-matching angles θ between 69° and 71.5° (Fig. 5); $\lambda_1 = \lambda_2$ (apex) thus corresponds to second-harmonic generation, and α denotes the non-collinear angle (Fig. 1). Phase matching can not be attained below the curve for non-critical collinear phase matching, $\alpha = 0°$.

In summary, we have shown that tunable UV radiation below 200 nm can be obtained with non-collinearly phase matched sum-frequency mixing of two flashlamp-pumped solid-state lasers, a tunable alexandrite laser and a fixed-frequency quadrupled Nd:YAG-laser, and we checked a theoretical model for the corresponding non-collinear phase-matching conditions at these wavelengths.

References

1. J. Ringling, O. Kittelmann, F. Noack: Opt. Lett. **17**, 1794 (1992)
2. K. Kato: Appl. Phys. Lett. **30**, 583 (1977)
3. Y. Tanaka, H. Kuroda, S. Shionoya: Opt. Commun. **41**, 434 (1982)
4. H. Hemmati, J. C. Bergquist, W. M. Itano: Opt. Lett. **8**, 73 (1983)
5. A. Borsutzky, R. Brünger, R. Wallenstein: Appl. Phys. B **52**, 380 (1991)
6. W. L. Glab, J. P. Hessler: Appl. Opt. **26**, 3181 (1987)
7. W. Mückenheim, P. Lokai, B. Burghardt, D. Basting: Appl. Phys. B **45**, 259 (1988)
8. M. Wanatabe, K. Hayasaka, H. Imajo, S. Urabe: Opt. Lett. **17**, 46 (1992)
9. T. Meguro, T. Caughey, L. Wolf, Y. Aoyagi: Opt. Lett. **19**, 102 (1994)
10. J. A. Giordmaine: Phys. Rev. Lett. **8**, 19 (1962)
11. S. Umegaki, S. Tanaka: Jpn. J. Appl. Phys. **16**, 775 (1977)
12. S. X. Dou, D. Josse, J. Zyss: J. Opt. Soc. Am. B **9**, 687 (1992)
13. S. X. Dou, D. Josse, R. Hierle, J. Zyss: J. Opt. Soc. Am. B **8**, 1732 (1991)
14. S. X. Dou, D. Josse, J. Zyss: J. Opt. Soc. Am. B **9**, 1312 (1992)
15. T. Hofmann, K. Mossavi, F. K. Tittel: Opt. Lett. **17**, 1691 (1992)
16. R. Danielius, A. Piskarsas, A. Stabinis, G. P. Banfi, P. Di Trapani, R. Righini: J. Opt. Soc. Am. B **10**, 2222 (1993)
17. L. A. W. Gloster, I. T. McKinnie, T. A. King: Opt. Commun. **112**, 328 (1994)
    L. A. W. Gloster, Z. X. Jiang, T. A. King: IEEE J. QE-**30**, 2961 (1994)
18. G. C. Bhar, U. Chaterjee: Jpn. J. Appl. Phys. **29**, 1103 (1990)
19. G. C. Bhar, U. Chaterjee, S. Das: Jpn. J. Appl. Phys. **29**, L1126 (1990)
20. G. C. Bhar, U. Chaterjee, S. Das: Opt. Commun. **80**, 381 (1991)
21. D. Eimerl, L. Davis, S. Velsko, E. K. Graham, A. Zalkin: J. Appl. Phys. **62**, 1968 (1987)

This article was processed by the author using the LaTeX style file *pljour2* from Springer-Verlag.